TABLE IV (continued)

Function	θ	$(x_1/x)^2$	$(x_2/x)^2$	$(x /x)^2$	Numerical value$\times 10^6$	Function	θ	$(x_1/x)^2$	$(x_2/x)^2$	$(x /x)^2$	Numerical value$\times 10^6$
$4\Delta_{ab}{}^2\Delta_{bc}\mathfrak{X}(x_1,x_2,x_3)$	60°	1	1	3/4	1225	$4\Delta_{ab}{}^2\Delta_{bc}\mathfrak{X}(x_1,x_2,x_3)$	60°	1	1	3/4	+1225
$x_1=\beta R_{ac}$	90°	1	2	5/4	+232	$x_1=\beta R_{bc}$	90°	2	1	1/2	−24
$x_2=\beta R_{bc}$	109°28'	1	8/3	19/12	−13	$x_2=\beta R_{ac}$	109°28'	8/3	1	1/3	−65
$x_3=\beta R_{b(ac)}$	120°	1	3	7/4	−41	$x_3=\beta R_{a(bc)}$	120°	3	1	1/4	−115
	146°27'	1	11/3	25/12	−51		146°27'	11/3	1	1/12	−77
	180°	1	4	9/4	−57		180°	4	1	0	−67

functions $\mathfrak{G}$–$\mathfrak{X}$ [Eqs. (9)–(16) of the text] are collected for isosceles triangles abc of argon atoms. To simplify the notation the dimensionless nearest-neighbor distance $\beta R_{ab}=\beta R_{ac}$ is represented by x; the numerical results for the auxiliary functions correspond with $x=2.5$.

Polar Reflection Faraday Effect in Metals*

EDWARD A. STERN,† JAMES C. McGRODDY, AND WILLIAM E. HARTE‡
University of Maryland, College Park, Maryland
(Received 30 August 1963; revised manuscript received 28 April 1964)

If one reflects plane-polarized light from a nonferromagnetic metal with a magnetic field normal to the reflecting surface, the reflected light is found to have its plane of polarization rotated from that of the incident beam, and is slightly elliptically polarized. This effect is known as the polar reflection Faraday effect (PRFE). The PRFE has been measured for aluminum and silver as a function of wavelength in the range 4150–8000 Å. The equipment to measure this effect to an accuracy of about 2% is described. Detailed studies on aluminum have shown that the PRFE is much less sensitive to the condition of the surface than ordinary optical-constant measurements and the measurements presented appear to be representative of bulk properties. The frequency dependence found for both aluminum and silver can in large part be explained by the simple intra-band theory. Although the theory relates the PRFE to the off-diagonal term of the conductivity tensor, the inconsistency of the many optical measurements of aluminum makes the determination of the off-diagonal conductivity ambiguous. In the case of silver, the real and imaginary parts of the off-diagonal conductivity can be obtained with a fair degree of accuracy.

I. INTRODUCTION

IT has been well known for quite some time that plane-polarized light after reflection from ferromagnetic metals magnetized normal to the reflection plane becomes elliptically polarized with its major axis rotated from the initial polarization direction.[1] The angle of rotation of this magneto-optic Kerr effect is of the order of one degree, and it is caused by the spin-orbit interaction.[2] Less well known and certainly not as intensely studied experimentally is an experimentally similar effect in nonferromagnetic metals which we call the polar reflection Faraday effect. Plane-polarized light

incident normally on a nonferromagnetic metal surface with a magnetic field normal to the surface, suffers on reflection a small rotation of the plane of polarization and also becomes slightly elliptically polarized. The reason why this effect has not been well studied experimentally is not hard to surmise when one realizes that the angle of rotation is about 10^{-4} deg for a field of 10^3 Oe. The amount of an elliptical polarization is also correspondingly smaller. In a rather remarkable bit of work, especially considering the experimental techniques available at that time, Majorana was apparently the first one to measure the polar reflection Faraday effect, doing so for Al, Ag, Au, Pt, Bi.[3] His accuracy was understandingly poor but he unquestionably showed the existence of the effect. Later and independently the effect was rediscovered and measured with greater accuracy taking advantage of the more modern techniques available.[4,5]

---

[1] F. A. Jenkins and H. E. White, *Fundamentals of Optics* (McGraw-Hill Book Company, Inc., New York, 1957), 3rd ed., Chap. 9.

[2] P. N. Argyres, Phys. Rev. 97, 334 (1955).

[3] Q. Majorana, Nuovo Cimento 2, 1 (1944).

[4] E. A. Stern and R. D. Myers, Bull. Am. Phys. Soc. 3, 416 (1958).

[5] E. A. Stern, Bull. Am. Phys. Soc. 5, 150 (1960); J. C. McGroddy and E. A. Stern, ibid. 8, 392 (1963).

In semiconductors the Faraday effect has been used to obtain useful information on the effective masses of the carriers.[6-8] Semiconductors are transparent to the electromagnetic radiation of interest and the Faraday effect is measured in transmission. Metals are not transparent to visible light, except for very thin films, and it is more favorable to measure the Faraday effect on reflection. Even in this most favorable case the effect is very small.

The motive for undertaking such a difficult measurement is that the polar reflection Faraday effect can, under certain conditions, be related to the properties of the Fermi surface of the metal being measured.[5,6,9] Unlike the magneto-optic Kerr effect, the polar reflection Faraday effect in nonferromagnetic metals is primarily produced by the orbital motion of the electrons as affected by the external magnetic field and the incident light. Because of the relatively high frequency of the incident light, collision effects with the lattice are relatively small, even for alloys at room temperature and the interpretation of the effect in terms of the properties of the Fermi surface is greatly simplified. In the next section the theory of the effect is discussed. Section III describes the experimental setup used to measure the effect while Sec. IV gives the experimental results for Al and Ag. Section V presents a discussion of the results and a comparison with theory.

II. THEORY

The presentation of the theory of the polar reflection Faraday effect (PRFE) can conveniently be split into two parts. The first part expresses the effect in terms of the dielectric tensor of the metal and the second part expresses the elements of the tensor in terms of the band structure of the metal.

We consider the case of a cubic metal only. When a magnetic field is applied in the z direction, the dielectric constant changes from a scalar to the following tensor form

$$\epsilon = \begin{bmatrix} \epsilon_{xx} & \epsilon_{xy} & 0 \\ -\epsilon_{xy} & \epsilon_{xx} & 0 \\ 0 & 0 & \epsilon_{zz} \end{bmatrix} . \qquad (1)$$

The ϵ in (1) includes all effects of the conduction electrons. It is related to the conductivity of the metal σ by

$$\epsilon_{ij} = \epsilon_{ij}{}^0 + i(4\pi\sigma_{ij}/\omega). \qquad (2)$$

Here i and j can be x, y, or z, $\epsilon_{ij}{}^0$ is the dielectric constant of the ion cores alone, and ω is 2π times the frequency of the electromagnetic radiation. It is assumed

that ϵ is only a function of ω and the dependence on wave number of the light is negligible. This is the usual dipole approximation.

At optical frequencies the effect of magnetic fields on ϵ is small and only the first-order effect of H need be considered. In this case (1) can be written

$$\epsilon = \begin{bmatrix} \epsilon_0 & \epsilon_1 & 0 \\ -\epsilon_1 & \epsilon_0 & 0 \\ 0 & 0 & \epsilon_0 \end{bmatrix} , \qquad (3)$$

where ϵ_0 is the dielectric constant at $H=0$ and ϵ_1 is ϵ_{xy} to first order in H.

To calculate the PRFE is a straightforward and tedious application of Maxwell's equations. The reflection can be expressed as a matrix such that

$$\begin{pmatrix} R_s \\ R_p \end{pmatrix} = \begin{pmatrix} r_{11} & r_{12} \\ r_{21} & r_{22} \end{pmatrix} \begin{pmatrix} I_s \\ I_p \end{pmatrix} , \qquad (4)$$

where R_s and R_p are the s and p components of the reflected electric vector, and I_s and I_p are the s and p components of the incident electric field. If we denote the angle of incidence by θ, the result to first order in ϵ_1/ϵ_0 is[10,11]

$$r_{11} = \frac{\cos\theta - (\epsilon_0 - \sin^2\theta)^{1/2}}{\cos\theta + (\epsilon_0 - \sin^2\theta)^{1/2}} ,$$

$$r_{22} = \frac{\epsilon_0 \cos\theta - (\epsilon_0 - \sin^2\theta)^{1/2}}{\epsilon_0 \cos\theta + (\epsilon_0 - \sin^2\theta)^{1/2}} ,$$

$$r_{12} = r_{21} = r_{11} \left\{ \frac{\epsilon_1}{(\epsilon_0 - 1)[(\sin^2\theta/\cos\theta) + (\epsilon_0 - \sin^2\theta)^{1/2}]} \right\} ,$$

$$= r_{22} \left\{ \frac{\epsilon_1}{(\epsilon_0 - 1)[(\sin^2\theta/\cos\theta) - (\epsilon_0 - \sin^2\theta)^{1/2}]} \right\} .$$

$$(5)$$

The square root appearing in (5) is defined by

$$(\epsilon_0 - \sin^2\theta)^{1/2} = a + ib, \qquad (5a)$$

where both a and b are positive. ϵ_0 is defined to have a positive imaginary part.

The PRFE rotation χ is defined by

$$\chi_s = \mathrm{Re}(r_{21}/r_{11}); \quad \chi_p = \mathrm{Re}(r_{21}/r_{22})$$

and the PRFE ellipticity by

$$Q_s = \mathrm{Im}(r_{21}/r_{11}); \quad Q_p = \mathrm{Im}(r_{21}/r_{22}), \qquad (6)$$

where Re means "real part of" and Im means "imaginary part of." Measurement of χ and Q permits the determination of ϵ_1 if ϵ_0 is known. Ordinary optical constants determine ϵ_0.

[6] M. J. Stephen and A. B. Lidiard, Phys. Chem. Solids 9, 43 (1959).
[7] T. S. Moss, S. D. Smith, and K. W. Taylor, Phys. Chem. Solids 8, 323 (1959).
[8] T. S. Moss, A. K. Walton, and B. Ellis, in *Proceedings of the International Conference on Physics of Semiconductors, Exeter* (The Institute of Physics and the Physical Society, London, 1962), p. 295.
[9] E. A. Stern, University of Maryland, Technical Report No. 261, 1962 (unpublished).

[10] N. Voigt, *Magnetooptik* (B. G. Teubner, Leipzig, 1908), pp. 694–702.
[11] T. Chang, R. C. Horsfall, and Edward A. Stern, University of Maryland Technical Report No. 245, 1962 (unpublished).

We now proceed to find an expression for ϵ_1 in terms of the band structure of the metal. We can define a new conductivity σ_1, which includes the effects of both the ion cores and conduction electrons by setting $\epsilon_{xy}{}^0 = 0$ in (2), obtaining

$$\epsilon_1 = i4\pi\sigma_1/\omega,\tag{7}$$

where σ_1 is first order in H. It has been shown that σ_{xy} and thus σ_1 satisfy the following dispersion relations,[12]

$$\sigma_1{}^{(r)}(\omega) = \frac{2}{\pi}\int_0^\infty \frac{x\sigma_1{}^{(i)}(x)dx}{x^2 - \omega^2}\tag{8}$$

and

$$\sigma_1{}^{(i)}(\omega) = \frac{-2\omega}{\pi}\int_0^\infty \frac{\sigma_1{}^{(r)}(x)dx}{x^2 - \omega^2},$$

where the principal value of the integrals are to be taken and $\sigma_1{}^{(r)}$ and $\sigma_1{}^{(i)}$ are the real and imaginary parts of σ_1, respectively. These dispersion relations permit one to calculate σ_1 if either the real or imaginary part alone is known for all frequencies.

Consider the propagation of circularly polarized light along H. It is easily shown that the induced currents are also circularly polarized and the conductivity of the metal for the circularly polarized light is a scalar given by

$$\sigma_\pm = \sigma_0 \pm i\sigma_1,\tag{9}$$

where the $+$ and $-$ signs refer to right and left circularly polarized light, respectively, and σ_0 is the conductivity of the metal at $H = 0$. The absorption of the circularly polarized light is proportional to the real part of $\sigma_\pm$. A physical interpretation of $\sigma_1{}^{(i)}$ is therefore that it is proportional to the difference in absorption between left and right circularly polarized light. This fact permits us to classify the various contributions to σ_1. The absorption of a photon corresponds to an electron making a transition from one state to another. If this transition is within the same band we call this an intraband effect. If the transition is from one band to another we call this an interband effect. Once we have classified these absorptions which determine $\sigma_1{}^{(i)}$ as interband or intraband, then by the dispersion relations (8) we can find the interband and intraband contributions of $\sigma_1{}^{(i)}$ to $\sigma_1{}^{(r)}$. By this means we can uniquely label the interband and intraband contributions to σ_1.

The intraband contribution to σ_1 is given by[6]

$$\sigma_1{}^{(a)} = \frac{e^3 I H}{4\pi^3\hbar^4 c[\omega + (i/\tau)]^2},\tag{10}$$

where

$$I = \int_{FS}\left[\left(\frac{\partial E}{\partial k_x}\right)\frac{\partial^2 E}{\partial k_y{}^2} - \frac{\partial E}{\partial k_y}\frac{\partial^2 E}{\partial k_y \partial k_x}\right]dk_y dk_z.$$

[12] H. S. Bennett and E. A. Stern, Bull. Am. Phys. Soc. 5, 279 (1960); H. S. Bennett and E. A. Stern, University of Maryland Technical Report No. 197, 1960 (unpublished); L. M. Roth, Phys. Rev. 133, A542 (1964); I. M. Boswarva, R. E. Howard, and A. B. Lidiard, Proc. Roy. Soc. (London) A269 125 (1962); E. A. Stern and H. S. Bennett (to be published).

Here the integral is over the Fermi surface, $E(\mathbf{k})$ is the energy of an electron in the Bloch state of wave vector $\mathbf{k}$, e is the electronic charge, and it is assumed that the collisions with the lattice can be accounted for by a relaxation time τ depending only on energy. The integral I can be rewritten in other forms that emphasize geometric properties[5,9]:

$$I = \tfrac{1}{2}\hbar^2 \oint dk_t \int dk_z \frac{v_\perp{}^2}{\rho_\perp},\tag{11a}$$

$$= \tfrac{1}{2}\hbar^2 \oint d\phi \int dk_z v_\perp{}^2,\tag{11b}$$

$$= \tfrac{3}{2}\hbar^2 \int_{FS} v^2\left(\frac{1}{\rho_1} + \frac{1}{\rho_2}\right)dS.\tag{11c}$$

In the above equations k_t is the component of the wave vector tangent to the curve determined by the intersection of the Fermi surface and a plane normal to the z direction; $v_\perp$ is the magnitude of the component of velocity along the curve in its own plane; $\rho_\perp$ is the radius of curvature of the curve in its own plane; ϕ is the angle between the normal to the curve and a fixed direction; v is the magnitude of the velocity on the Fermi surface; ρ_1 and ρ_2 are the two principal radii of curvature of the Fermi surface; dS is an element of area on the Fermi surface; the first two integrals are around the curve and summed over all such curves; and the last integral is over the Fermi surface. We see from the form of I given in Eqs. (11) that $\sigma_1{}^{(a)}$ is proportional to an average centrifugal acceleration of the electron in the magnetic field.

The interband contribution to σ_1 can be written formally as[12]

$$\sigma_1{}^{(e)}(\omega) = \sigma_1{}^{(r,e)}(\omega) + i\sigma_1{}^{(i,e)}(\omega),$$

$$\sigma_1{}^{(i,e)}(\omega) = \frac{-\pi e^2}{4mV}$$

$$\times \sum_{n,l}\left[f_{nl}{}^+\delta(\omega_{nl} - \omega) - f_{nl}{}^-\delta(\omega_{nl} - \omega)\right],\tag{12}$$

$$\sigma_1{}^{(r,e)}(\omega) = \frac{-e^2}{2mV}\sum_{nl}\left[\frac{\omega_{nl}(f_{nl}{}^+ - f_{nl}{}^-)}{\omega_{nl}{}^2 - \omega^2}\right].$$

Here $\sigma_1{}^{(i,e)}(\omega)$ and $\sigma_1{}^{(r,e)}(\omega)$ denote the imaginary and real parts of the interband contribution to σ_1, respectively, m is the free-electron mass, V is the volume of the metal, l labels all filled states and n labels all unfilled states in the completely unfilled bands, $\hbar\omega_{nl}$ is the energy difference between states n minus states l. The principal value of the right-hand side of the second equation is to be taken while $\delta(x)$ is the Dirac delta function. The oscillator strengths for both right $(+)$ and left $(-)$ circularly polarized light $f_{nl}{}^\pm$ are defined

by

$$f_{nl}{}^{\pm} = |\pi_x \pm i\pi_y|_{nl}{}^2 / m\hbar\omega_{nl}. \tag{13}$$

Here (π/m) is the velocity operator given by $[\mathbf{p} - (e/c)\mathbf{A}]/m$, where $\mathbf{p}$ is the momentum operator and $\mathbf{A}$ is the vector potential of the external magnetic field. The notation $|\quad|_{nl}{}^2$ means the absolute square of the matrix element between states $\mathbf{l}$ and $\mathbf{n}$.

The formal forms for $\sigma_1{}^{(e)}$ given in (12) include the magnetic field effects to all orders. Since σ_1 was defined to depend on H to only the first power, we will assume that it is understood that the formal expression in (12) is subsequently expanded in powers of H and only the first power retained.

Finally, we point out that $\sigma_1{}^{(r)}$ and $\sigma_1{}^{(i)}$ satisfy the following rules[12]:

$$\lim_{\omega \to \infty} \sigma_1{}^{(r)}(\omega) = -\omega_p{}^2\omega_c/4\pi\omega^2, \tag{14}$$

and

$$\int_0^\infty x\sigma_1{}^{(i)}(x)dx = -\omega_p{}^2\omega_c/8,$$

where $\omega_p{}^2 = 4\pi n e^2/m$, $\omega_c = eH/mc$, and n is the number of electrons per unit volume.

An estimate of the expected angle of rotation χ on a free-electron model yields about 10^{-4} deg per 10^3 Oe at normal incidence. Unlike the case in transmission, this value is almost independent of the frequency for frequencies well below ω_p. It is possible to measure this small angle of rotation to a few percent accuracy as described in the next section.

In order to carry out these measurements it is convenient to reflect the light from the sample many times to amplify the PRFE. However, when this is done, a phase shift to be described below, is also introduced. Because this phase shift effect is utilized to measure both the real and the imaginary parts of (r_{21}/r_{11}), and hence of σ_1, a detailed account of it is given here.

The expressions given in (4) and (5) represent the effects of one reflection. If this same beam of light is reflected n times in a magnetic field from a mirror arrangement such as that shown in Fig. 1, the resulting effect will be complicated by the difference in phase change on reflection for s and p polarization. Thus, for example, the measured angle of rotation $\chi^{(n)}$ will not in general be simply $n\chi$, where χ is the angle of rotation after one reflection.

Consider an initially s-polarized wave incident on the specimen, the electric vector being perpendicular to the plane of the page. After the first reflection from the horizontal portions of the mirror system of Fig. 1, (at "a"), the PRFE produces in the reflected wave a very small amount of p polarization. That part of the p polarization in phase with the s polarization produces a rotation of the plane of polarization, while the p polarization 90° out of phase with the s polarization produces elliptical polarization of the reflected wave. After the next reflection (at point "b" in Fig. 1) the PRFE again
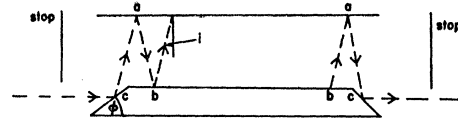

FIG. 1. Geometry of the samples used. Two types, I and II, were used. For type I, $\phi = 42.5°$, $i = 5°$, and the number of reflections, from the two parallel surfaces, $n = 21$. For type II, $\phi = 38°$, $i = 14°$, and $n = 17$. The points a, b, and c indicate the three different types of reflection.

produces in the reflected wave some additional p polarization, which adds to the p polarization already present in the incident wave. However, this p polarization which was present in the wave incident at "b" does not have the same phase after reflection at "b" as the p polarization produced in the second reflection because of the difference in phase angle change on reflection for s and p polarization. The problem is most easily treated by use of the matrices defined in Eqs. (4) and (5):

$$\begin{pmatrix} R_s \\ R_p \end{pmatrix} = \begin{pmatrix} r_{11} & r_{12} \\ r_{21} & r_{22} \end{pmatrix} \begin{pmatrix} I_s \\ I_p \end{pmatrix} = r \begin{pmatrix} I_s \\ I_p \end{pmatrix}. \tag{4}$$

The diagonal elements r_{11} and r_{22} are the ordinary Fresnel coefficients. The off-diagonal element r_{12} changes sign upon reversal of the direction of surface normal with respect to the magnetic field. The effect of the entire sample on polarized light can be represented by a matrix

$$R = r(c)\{r(a)r(b)r(a) \cdots r(b)r(a)\}r(c),$$

where the brackets contain n factors of r. The matrix $r(c)$ represents reflection at points "c" in Fig. 1 and $r(a)$ and $r(b)$ represent reflections at points "a" and "b," respectively. The only difference between $r(b)$ and $r(a)$ is that the sign of r_{21} is reversed. The measured angle of rotation is given by

$$\chi_s{}^T = \mathrm{Re}(R_{21}/R_{11}). \tag{15}$$

It is a straightforward matter to calculate the elements of R. The result is approximately

$$\frac{R_{21}}{R_{11}} = \frac{r_{12}(a)}{r_{11}(a)}(n + 2\cos\phi)e^{-i\Delta_T}, \tag{16}$$

where we have written

$$r_{22}(a)/r_{11}(a) = -e^{-i\Delta(a)} \tag{17}$$

and

$$\Delta_T = \frac{(n-1)}{2}\Delta(a) + \Delta(c)$$

in a straightforward notation.

To calibrate the apparatus, a gas of known Verdet constant[13] is introduced between the mirrors and the

[13] L. R. Ingersoll and D. H. Liebenberg, J. Opt. Soc. Am. **46**, 538 (1956).
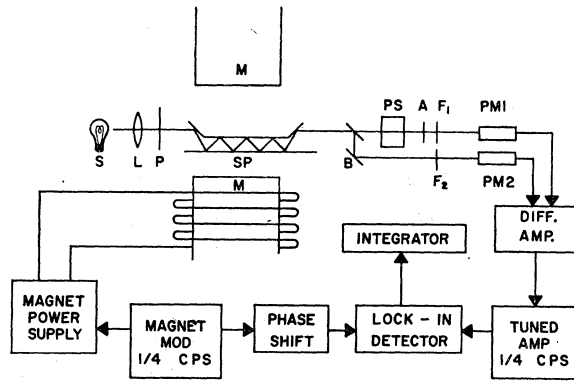
FIG. 2. Block diagram of the apparatus.

change in signal is measured. Using arguments similar to the above we obtain for the angle of rotation produced by the gas

$$X_g = X_0(n+1) \cos\Delta_T,$$

where X_0 is the rotation produced in one traversal between the two parallel mirrors. The ratio of the rotation due to the sample to that due to the gas is given by

$$\frac{X_s^T}{X_g} = \frac{(n+2\cos\phi)\,\mathrm{Re}[r_{12}(a)/r_{11}(a)]e^{-i\Delta_T}}{X_0(n+1)\cos\Delta_T}$$

which reduces to

$$\frac{X_s^T}{X_g} = \frac{(n+2\cos\phi)(X_s+Q_s\tan\Delta_T)}{(n+1)X_0}, \quad (18)$$

where

$$X_s = \mathrm{Re}[r_{21}(a)/r_{11}(a)]; \quad Q_s = \mathrm{Im}[r_{21}(a)/r_{11}(a)]$$

as before.

In the experiment the quantities measured are X_s^T/X_g and n, which is already known from the geometry of the sample. X_g can be calculated from the dimensions of the sample and known Verdet coefficients. Δ_T can be inferred from measured optical constants. By making measurements on the same sample for two different values of Δ_T the quantities X_s and Q_s can be determined. Using these and the optical constants $\sigma_1^{(r)}$ and $\sigma_1^{(i)}$ can be calculated. On value of Δ_T is obtained as explained above, while the value $\Delta_T=0$ is obtained by placing a phase shifting mirror of the same metal as the sample in a region where the magnetic field is small. This mirror is oriented so that the light is incident at a slightly larger angle of incidence than that at last end mirror of the sample, but rotated 90° so that p and s polarizations are reversed. This has the effect of multiplying the right side of Eqs. (16) and (18) by $e^{i\Delta_T}$, giving total phase shift zero.

The above discussion has considered the case of an initially s-polarized wave in conformity with the experimental setup used. A similar analysis can be performed for an initially p-polarized wave but will not be presented here, since such an arrangement was not used in the measurements.

III. EXPERIMENTAL APPARATUS

The method of measuring the PRFE is in principle simple. Polarized light after reflecting off the sample in a magnetic field passes through an analyzer set about 10° from minimum transmission. The magnetic field intensity is modulated, causing the plane of polarization of the light to oscillate slightly because of the PRFE. This oscillation is converted to an alternating component of light intensity by the analyzer and is detected by a photomultiplier tube. Because of the small signals involved it is necessary to refine the experimental technique so as to reach the absolute limit of the statistical noise of the finite number of photons per second being detected by the photomultiplier.

A block diagram of the apparatus is shown in Fig. 2. The light source S is a tungsten filament supplied from a regulated dc power supply. The lens L condenses the light which is then polarized with its electric field parallel to the mirror surface by a sheet polaroid. The plane-polarized light is then deflected by an end mirror to two parallel mirrors SP, where it reflects n times before reflecting off the other end mirror. The specimen mirrors SP are made by evaporating the metal to be studied on polished plate glass substrates. The specimen SP is placed between the poles M of an electromagnet. By reflecting the light back and forth n times, the angle of rotation due to the PRFE is increased by approximately this factor (n is either 17 or 21 as indicated in the caption to Fig. 1). After passing through the specimen the light is split by beam splitter B so that part of the light passes through phase shifter PS as described above and then through analyzer A, consisting of a sheet polarizer, filter F_1 and onto photomultiplier PM 1. The rest of the light passes through filter F_2 onto photomultiplier PM2.

An alternating current of $\frac{1}{4}$ cps is passed through the electromagnet by the magnet power supply and modulator. This produces an alternating magnetic field of about 10 000-Oe peak to peak between the poles M which causes a corresponding variation in the polarization direction of the light because of the PRFE in the specimen SP. The polarizer P and analyzer A are oriented with respect to one another about 10 deg from being crossed. The varying polarization direction is translated by the analyzer A into an intensity change at $\frac{1}{4}$ cps. Only PM 1 sees this intensity change produced by the PRFE. Photomultiplier PM 2 sees only intensity variations from other causes such as vibrations or source S variations. The outputs from PM 1 and 2 are fed into a difference amplifier whose output ideally is proportional to only PRFE. This output next proceeds to a tuned amplifier at $\frac{1}{4}$ cps and then into a lock-in detector. The reference signal of the lock-in detector comes from the magnet supply modulator and is, of

course, correlated with the desired signal. The output of the lock-in detector is fed into an integrator which effectively narrows the bandwidth even further. A typical integration time is 10 min. The calibration of the equipment is accomplished by admitting a known pressure of an appropriate gas between the two parallel mirrors of the specimen SP. The known Faraday effect in the gas[13] gives an additional signal which calibrates the equipment. During a measurement of the PRFE care is taken to evacuate the region between the mirrors to below 0.2 Torr in order that the Faraday effect in the residual gas does not produce an appreciable error. Any zero correction to the apparatus was determined by removing the specimen and measuring the residual signal. As a result, a correction ranging from 1 to 6% was applied to the data obtained from type I samples.

The photomultipliers PM 1 and 2 were magnetically shielded by at least two cylinders, one inside the other, of high magnetic permeability material. S 11 response photomultipliers were used to cover the range from 4150 to 6500 Å while the range from 6500 to 8000 Å was covered by an $S1$ response. The filters used have a half-width of about 3 or 4%. Because of the slow variation of the PRFE with wavelength this width caused negligible error.

Extreme care was taken to insure that the measured light intensity changes were due to only the PRFE and to no other cause. The use of two photomultipliers as described should cancel most other undesired signals. However, to make certain that only the PRFE was being measured, the analyzer was rotated to an equal angle on the opposite side of the minimum transmission position and the PRFE remeasured. For this new position the PRFE changes sign while all other contributions except one do not. The one spurious signal which does not change sign is the Faraday rotation in the glass parts of the beam splitter. This signal is measured separately as explained below. By this means undesired signals can be revealed, and, by taking the difference between the two measurements, eliminated. Such undesired signals were found, and although they were smaller than the PRFE, their source was also found. The two largest sources of the undesired signals were (a) the direct modulation of the photomultiplier outputs by the varying magnetic fields, and (b) misalignment of polarizer P. The effect (a) was caused by the fact that even the best magnetic shielding material has some hysteresis in it and can shield against magnetic field variations only done to a few mG, but no lower. This effect was eliminated by orienting the two photomultipliers with respect to one another such that the magnetic field variations in them were equal and cancelled out.

IV. EXPERIMENTAL RESULTS

In measuring the PRFE the same question that arises for any optical measurement naturally presents itself.
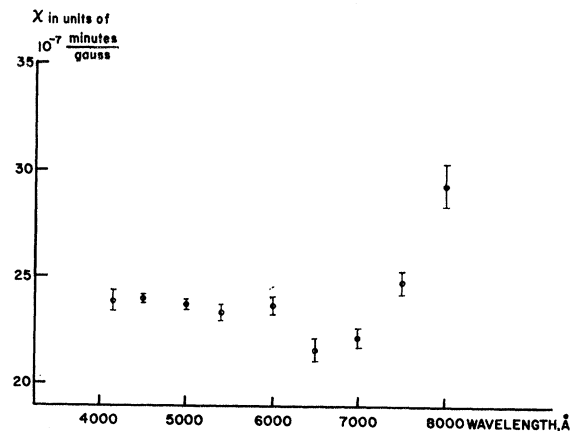

FIG. 3. Wavelength dependence of the PRFE rotation for an angle of incidence of 5° for Al.

Is the measurement characteristic of the bulk properties of the metal, or is it just a surface effect characteristic of the particular film being studied? This question was studied in great detail for aluminum.

In all cases the metal samples were evaporated in vacuum onto a glass substrate using a tungsten filament. They were removed from the evaporator and exposed to the atmosphere during preparation for the measuring equipment. Films prepared in such a manner are polycrystalline. However, in cubic crystals σ_1 is independent of orientation of the crystal, and thus a polycrystalline sample gives as much information as a single-crystal sample.

Exposure of the aluminum sample to the atmosphere causes the build-up of a layer of Al_2O_3, transparent in the visible, which does not exceed about 40 Å. The build-up of the oxide layer is initially rapid, reaching a thickness of 30 Å after about 24-h exposure to the atmosphere. The terminal thickness is reached after about a month. Measurements on the same sample from a few hours after evaporation to periods on the order of a month later revealed no measureable difference in the case of aluminum for either type-I or -II samples. To confirm this result a theoretical estimate of the effect of a 40-Å oxide layer was made and found to be only 1 or 2%. It was concluded that the Al_2O_3 layer produces no appreciable effect.

The effect of the method of preparation of the films was also studied. Films were evaporated in residual vacuums of 10^{-1} to 5×10^{-7} Torr for type-II samples and 5×10^{-6} to 2×10^{-7} Torr for type-I samples. The residual gasses were, in all cases but one, those remaining from the atmosphere. In the one exception the evaporator had been flushed with argon before evaporation at pressures around 10^{-1} Torr. The largest variation from sample to sample was just outside the experimental uncertainties for type-I samples, and there was no variation from sample to sample for type-II samples within the experimental error of a few percent. The
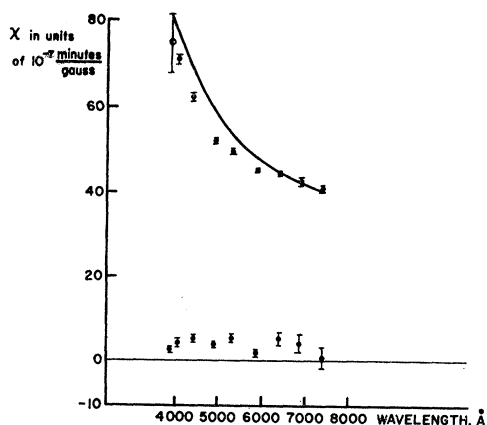
FIG. 4. Wavelength dependence of the PRFE rotation (upper points) and ellipticity (lower points) for silver for an angle of incidence of 5°. The solid curve is calculated from Eqs. (5) and (10) with $\omega\tau\gg1$ and using the optical constants of Schulz and Tangherlini, with I as a parameter.

optical constants of several of the samples were measured using the Drude polarimetric method, and were found to be within approximately 10% of those measured by Schulz and Tangherlini.[14,15] There is a significant variation in the optical constants, but no such significant variation in the PRFE was found. On the basis of the above measurements it was concluded that the PRFE for Al as measured is characteristic of the bulk. In all samples but two, the aluminum had a stated purity of 99.99%. For two type-II samples the purity was 99%.

The measured values of the rotation X_s for an angle of incidence of 5° are plotted in Fig. 3, and tabulated in the table. The errors quoted are standard deviations calculated from the measurements on three type-I specimens. These errors reflect not only the reproducibility of the measurements, but also the consistency between differently prepared specimens. As can be seen, the results emphasize the conclusion discussed previously of how insensitive the PRFE is to the condition of the evaporated film. The PRFE rotation can be measured more reproducibly than the optical constants, which are more sensitive to the condition of the film. The errors plotted in Fig. 3 do not reflect errors in the absolute calibration of the apparatus, estimated to be 1 or 2%.

In the case of silver, not such extensive checks were made to determine if the results were characteristic of the bulk. Thus the results for silver cannot be considered to be as reliable as those for aluminum. However, the room temperature results for silver, plotted in Fig. 4 and tabulated in the table for a type-I sample illustrate that the effect measured is a function of the specimen and is not characteristic of the equipment because of

[14] L. G. Schulz, J. Opt. Soc. Am. 44, 357 (1954).
[15] L. G. Schulz and F. R. Tangherlini, J. Opt. Soc. Am. 44, 362 (1954).

the different wavelength dependence. The purity of the silver used was at least 99.99%. The solid curve is the wavelength dependence expected based on an intraband model using the optical constants of Schulz and Tangherlini. The parameter I_{FS} was chosen to fit the data at 7000 Å.

In both aluminum and silver the sense of rotation is the same as that in the Faraday effect in the gas used for calibration, which for aluminum was usually oxygen, and for silver was nitrogen. This means that $\sigma_1{}^r$ has the same sign for aluminum and silver as for oxygen, which corresponds to negatively charged carriers. The PRFE rotation in both Al and Ag has the opposite sign from that found in the magneto-optic Kerr effect in iron. Verification that the PRFE is linear in the magnetic field was also made. This again is in contrast to the magneto-optic Kerr effect, which is proportional to the magnetization of the ferromagnet.[2]

The rotation measured with $\Delta_T\neq0$ is in most cases quite close to that for $\Delta_T=0$, the pure PRFE rotation. Thus, the values of Q_s are in general quite small, and the relative error in Q_s is much larger than that in X_s.

V. DISCUSSION OF RESULTS

The quantities measured in this experiment were the real and imaginary parts of (r_{21}/r_{11}), which is related to the off-diagonal conductivity by Eq. (5). In order to interpret the data in terms of the band structure of a metal it is necessary to be able to effect a separation of σ_1 into inter- and intraband contributions. The calculations of the real and imaginary parts of σ_1 from the experimental results requires a knowledge of the optical constants.
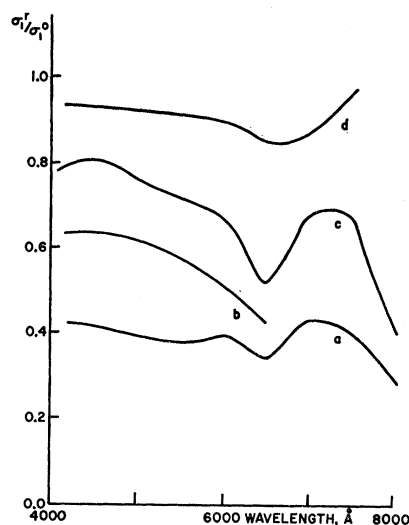

FIG. 5. Wavelength dependence of the real part of the off-diagonal conductivity for aluminum. The various curves correspond to different optical constants. Curve "a" is for the optical constants of Schulz and Tangherlini. Curve "b" is for the optical constants of Hass and Waylonis. Curve "c" is for the optical constants of Ehrenreich, Philipp and Segall. Curve "d" is for the optical constants derived from a free-electron model with $\omega\tau\gg1$.

TABLE I. Units are 10^{-7} min/G.

Wavelength (angstroms)	Aluminum			Silver		
	PRFE rotation χ_s	Majorana result	PRFE ellipticity Q_s	PRFE rotation χ_s	Majorana result	PRFE ellipticity Q_s
4000	...		...	74.9 ±7.5		2.1±0.65
4150	23.9 ±0.45	31±7	−1.9±1.1	70.9 ±0.8	85±17	4.0±1.1
4500	24.0 ±0.20		0.7±1.2	61.6 ±0.8		4.9±1.2
5000	23.75±0.25		−0.4±1.0	51.7 ±0.2		3.6±0.7
5400	23.4 ±0.35		−1.4±1.2	49.0 ±0.2		5.0±1.1
6000	23.7 ±0.4		−2.7±1.5	44.15±0.1		0.9±1.2
6500	21.65±0.55		−5.4±2.4	43.7 ±0.5		4.8±1.5
7000	22.2 ±0.45		5.6±2.0	41.8 ±0.9		3.5±2.5
7500	24.8 ±0.55		7.0±3.0	40.05±0.8		1.0±2.8
8000	30.4 ±1.0		...	...		...

The optical constants of aluminum have been studied by a number of authors.[14-21] Direct measurements of the optical constants of aluminum in the visible have been carried out by Schulz and Tangherlini,[14,15] and by Hass and Waylonis.[20] In addition extensive reflectance measurements have been made by Bennett, Silver, and Ashley,[21] and by Madden, Canfield, and Hass.[16] The reflectance data have been analyzed by a Kramers–Kronig procedure by Ehrenreich, Philipp, and Segall[19] to yield optical constants. The various results differ from one another by 10–20%. Although measurements of the topolgical features of the Fermi surface of alumi-
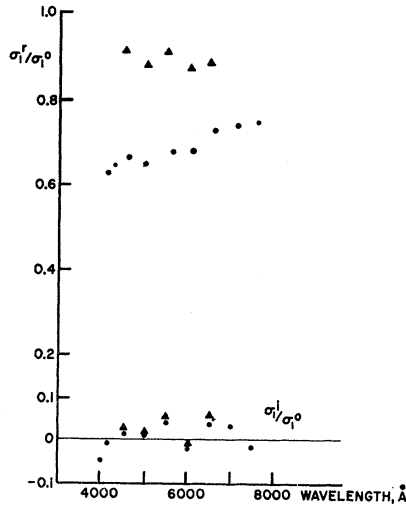

FIG. 6. Wavelength dependence of the real and imaginary parts of the off-diagonal conductivity for silver. The upper points of each pair are for the optical constants of Otter. The lower points are for the optical constants of Schulz and Tangherlini.

num by other methods,[22] notably the de Haas–van Alphen effect and the magnetoacoustic effect, and a number of independent band-structure calculations all lead to a nearly free-electron structure, the optical data do not agree with this result. The reasons for this are not understood. The PRFE data on aluminum have been analyzed using Eq. (5) using optical constants from several sources. The resulting spectra of σ_1 as a function of wavelength are shown in Fig. 5. All values have been plotted in units of the free-electron off-diagonal conductivity given by the first of Eqs. (14). It is clear that the optical constants of aluminum are not sufficiently well known to pernit an accurate determination of σ_1. It is of some interest to note that in the wavelength region below the absorption at 8500 Å the results are in reasonable agreement with what one would expect on the basis of a nearly free electron model if one uses free-electron optical constants.

In the case of silver, although not very extensive measurements have been performed, a sketch of the results of a similar analysis is given in Fig. 6. The optical constants for silver differ less from one worker to another, although recent results reported by Otter[23] on samples prepared by a new method are much more free-electron like than previous results.[14,15] It is clear from the fact that the imaginary part of σ_1 is very small that interband effects only play at most an indirect role. Silver has a strong absorption at about 3300 Å,[24] and the wavelength dependence of the contribution to $\sigma_1^r(\omega)$ due to structure in $\sigma_1^i(\omega)$ at that wavelength can be calculated from the dispersion relations (8). This enables one to estimate the importance of such effects on the spectrum of $\sigma_1^r(\omega)$ shown in Fig. 6. Such effects are clearly quite small. Additional measurements on silver and gold are now being carried out in this laboratory.

Agreement with the simple intraband theory is indicated by the ratio σ_1^r/σ_1^0 being independent of fre-

[16] R. Madden, L. Canfield, and G. Hass, J. Opt. Soc. Am. **53**, 620 (1963).

[17] J. Hodgson, Proc. Roy. Soc. (London) **B68**, 593 (1955).

[18] J. R. Beattie and G. K. T. Conn, Phil Mag. **46**, 989 (1955).

[19] H. Ehrenreich, H. R. Philipp, and B. Segall, Phys. Rev. **132**, 1918 (1963); and H. R. Philipp (private communication).

[20] G. Hass and J. E. Wayolnis, J. Opt. Soc. Am. **51**, p. 719 (1961).

[21] H. E. Bennett, M. Silver, and E. J. Ashley, J. Opt. Soc. Am. **53**, 1089 (1963).

[22] For a list of references see the paper by G. N. Kamm and H. V. Bohm, Phys. Rev. **131**, 111 (1963).

[23] M. Otter, Z. Physik **161**, 163 (1961).

[24] H. Ehrenreich and H. R. Philipp, Phys. Rev. **128**, 1622 (1962).

quency if $\omega\tau \gg 1$. If $\omega\tau$ is not much greater than one, then one expects a variation of σ_1^r/σ_1^0 with wavelength. Interband effects also will produce a variation of σ_1^r/σ_1^0 with wavelength. For Ag over the range measured, $\omega\tau \gg 1$, while for Al one expects $\omega\tau$ effects to start producing a variation in σ_1^r/σ_1^0 near the long-wavelength end of the measured region.

The only previous experimental measurements to compare the measurements with are those of Majorana. Majorana used a tungsten light source and a Na photocathode. This combination has a peak sensitivity centered around 4500 Å. Table I shows the Majorana values χ, which are in reasonable agreement with our measurements in the vicinity of 4500 Å.

VI. CONCLUSIONS

In this paper the first detailed study of the PRFE in aluminum and silver has been presented. It has been found possible to measure the effect with an accuracy of a few percent. Arguments have been presented indicating, at least for Al, that the property measured is characteristic of the bulk. The determination of the real and imaginary parts of σ_1 for Al has not been possible because the optical constants are not known with sufficient accuracy. For Ag the results are in reasonable agreement with the intraband theory.

ACKNOWLEDGMENTS

High-Temperature Susceptibility of Heisenberg Ferromagnets Having First- and Second-Neighbor Interactions*

PETER J. WOJTOWICZ

RCA Laboratories, Princeton, New Jersey

AND

R. I. JOSEPH

Raytheon Research Division, Waltham, Massachusetts

(Received 5 March 1964)

Exact power-series expansion of the high-temperature magnetic susceptibility of the nearest-neighbor Heisenberg ferromagnets have been provided by Rushbrooke and Wood. This paper describes the derivation of high-temperature susceptibility series for Heisenberg ferromagnets having both first- and second-neighbor exchange. The calculation is accomplished by extending the general diagrammatic technique developed by Rushbrooke and Wood to include the second-neighbor interaction. All mixed coefficients for terms through the fourth power of the inverse temperature have been computed for arbitrary spin and general lattice structure. The series expansions have been applied to the susceptibility of gadolinium in order to determine the quality of information which can be obtained from experimental data. It is found that the susceptibility is not quite sensitive enough to be able to specify the values of both the first- and second-neighbor exchange constants. It is shown, however, that the theory is capable of providing one definite relationship between the values of the two constants. The determination of unique values for the constants then requires the analysis of additional experimental data. The value of the Curie constant is uniquely specified.

I. INTRODUCTION

THE theory of the high-temperature susceptibility of the Heisenberg model ferromagnets has been advanced to a high degree of approximation through the extensive development of the exact power-series expansion method of Kramers and Opechowski[1] by Rushbrooke and Wood[2] (their paper shall henceforth be denoted by R-W). With this technique the susceptibility is expressed as a Taylor series in ascending powers of the reciprocal temperature. The coefficients of the series are then evaluated using a systematic and powerful diagrammatic analysis. All coefficients through the sixth-power term have been computed in R-W for general spin and arbitrary lattices. These six coefficients have been further generalized by Morgan and Rushbrooke[3] to include the concentration dependence in ferromagnets containing random admixtures of nonmagnetic elements.

* This research was independently supported by the RCA Laboratories and the Raytheon Research Division.

[1] W. Opechowski, Physica 4, 181 (1937); 6, 1112 (1938).

[2] G. S. Rushbrooke and P. J. Wood, Mol. Phys. 1, 257 (1958); denoted by R-W in the text.

[3] D. J. Morgan and G. S. Rushbrooke, Mol. Phys. 4, 291 (1961).